

# Schwann cells modulate short-term plasticity of cholinergic autaptic synapses

Anna P. Perez-Gonzalez, David Albrecht, Juan Blasi and Artur Llobet

Laboratori de Neurobiologia – CIBERNED, IDIBELL – Universitat de Barcelona, 08907 L'Hospitalet de Llobregat, Spain

Nicotinic synapses in the autonomous nervous system display use-dependent plasticity but the contribution of cellular environment, as well as the presynaptic mechanisms implicated in this process remain to be determined. To address these questions synaptic function was assayed in rat superior cervical ganglion (SCG) neurons microcultured in isolation from any other cell type and compared to those microcultured in the presence of Schwann cells of ganglionic origin. Schwann cells were not required for synapse formation *in vitro* because functional cholinergic autaptic synapses were established in both experimental conditions. The number of synapses was comparable between the two culture conditions but the frequency of spontaneous miniature excitatory postsynaptic currents was enhanced in those neurons grown in direct contact with glial cells. Autapses displayed facilitation and depression, both processes being determined by the fraction of vesicles from the readily releasable pool discharged by an action potential. At high release probabilities vesicles were more efficiently mobilized, thus promoting depression, whilst low release probabilities made facilitation likely to occur. Schwann cells did not modify significantly facilitation but increased synaptic depression. In single cell microcultures, paired pulse stimuli showed a monoexponential recovery from depression with a time constant of ~60 ms, while in microcultures developed together with glial cells, recovery was bi-exponential with a significantly slower time course. Altogether these results show that Schwann cells from sympathetic ganglia directly modulate use-dependent plasticity of nicotinic synapses *in vitro* by enhancing short-term depression.

(Received 18 July 2008; accepted after revision 7 August 2008; first published online 14 August 2008)

**Corresponding author** A. Llobet: Laboratori de Neurobiologia – CIBERNED, IDIBELL – Universitat de Barcelona, 08907 L'Hospitalet de Llobregat, Spain. Email: allobet@ub.edu

A key process for information processing in neurons is homosynaptic short-term plasticity, which takes place when repeated firing of a presynaptic neuron induces a change in synaptic efficacy (Dittman & Regehr, 1998; Millar *et al.* 2002; Zucker & Regehr, 2002). Increasing evidence indicates that glial cells are active modulators of use-dependent plasticity. For example, in the neuromuscular junction perisynaptic Schwann cells are key to determining the degree of high frequency induced depression (Robitaille, 1998), and in hippocampal synapses synaptic suppression is mediated by astrocytes (Zhang *et al.* 2003). In addition, glial cells are required for multiple neuronal functions, ranging from development and establishment of synapses (Christopherson *et al.* 2005) to buffering of neurotransmitters (Mennerick & Zorumski, 1994), protons (Deitmer & Rose, 1996) or potassium (Kofuji & Newman, 2004).

One of the key elements that determine glial actions on neuronal function is their tight location to neuronal processes, as for example Schwann cells at the neuromuscular junction or Bergmann glia at the cerebellum. However, such structural organization is the result of a developmental process, which cannot be modified without compromising synaptic function. In order to overcome this limitation, the aim of the present study was to set up an *in vitro* approach where neuronal development was essentially determined by the composition of the culture medium, thus compensating the direct trophic actions of the cellular environment. Ideally, under such experimental conditions, glial cells should also be able to establish interactions with neurons *in vitro* similar to those present *in vivo*. Hence, this type of approach would make it possible to separate the participation of neuron–glia interactions on synaptic plasticity from their developmental role.

Neuronal microcultures provide a simple scenario to study synaptic function, because a given neuron is both

This paper has online supplemental material.

presynaptic and postsynaptic since it is forming a network of autaptic contacts (Furshpan *et al.* 1986b; Bekkers & Stevens, 1991). Autapses resemble their synaptic counterparts and display multiple plasticity features (Goda & Stevens, 1998; Schluter *et al.* 2006), so microcultures offer an accessible, direct approach for identifying the molecular mechanisms underlying short-term plasticity (Murthy *et al.* 1997). Glial secreted products, however, are essential to establish successful microcultures from central neurons, because it has been demonstrated that in their absence there are a very low number of functional synapses formed (Nagler *et al.* 2001). In contrast, some neurons from the peripheral nervous system show less complex trophic requirements. Sympathetic neurons are an example, because their survival and development are essentially dependent on nerve growth factor (NGF) both *in vivo* and *in vitro*. For this reason, in the present study we microcultured sympathetic neurons from the superior cervical ganglion (SCG), modifying procedures already described (Furshpan *et al.* 1986b).

By using the experimental conditions hereby explained, short-term plasticity displayed by synapses where only the pre- and postsynaptic elements were present was compared to those where Schwann cells of sympathetic origin coexisted throughout the microculture procedure. The results obtained showed that this particular type of glial cell had a specific effect both on the frequency of spontaneous miniature postsynaptic currents (mEPSCs) and on short-term depression, thus reinforcing the idea that short-term plasticity is tightly coupled to the cellular environment.

## Methods

### Animals

Albino Sprague–Dawley rats (P0–P2) were used for preparation of superior cervical ganglia. Animals were chilled in ice. Once surgery was finished, pups were killed by decapitation. The procedure was approved by the ethical committee of Generalitat de Catalunya (DMA no. 3326).

### Establishment of single cell microcultures from rat superior cervical ganglion neurons

To prepare microcultures, sterilized coverslips (15 mm diameter) were placed in a 12-well plastic dish and covered with a thin agarose layer (0.15%). The agarose was left to dry for at least 1 h under UV light. Collagen was prepared from rat tails and stored at 4°C in an acidic medium for no longer than 5 months. Microdots were fabricated using a perfume atomizer immediately before plating the neurons. The pH of collagen was adjusted to a moderate basic value

(7.5–8) when sprayed and viscosity was assayed for the different stocks before use.

The essential procedure for isolation and culture of SCG neurons was performed using protocols described elsewhere (Mains & Patterson, 1973; Furshpan *et al.* 1986b). Neurons were dissociated from the superior cervical ganglia of newborn albino Sprague–Dawley rats (P0–P2). At least 20 ganglia were used in each culture. Ganglia were enzymatically treated at 37°C, first with 2.5 mg ml<sup>-1</sup> collagenase (Sigma-Aldrich, St Louis, MO, USA) for 10 min, followed by 0.05% trypsin–EDTA solution (Invitrogen, Carlsbad, CA, USA) for 20 min. Trypsin was removed and ganglia were placed in a high serum medium based on Dulbecco's modified Eagle's medium (DMEM)–F12 (1 : 1) + 20% fetal bovine serum (FBS) (Invitrogen) to ensure inactivation of the remaining enzyme. Complete disaggregation was achieved mechanically using sterilized glass pipettes. Dissociated neurons were then placed in a 10 cm culture dish and kept for ~90 min in the incubator. This preplate period allowed non-neuronal cells to attach to the culture dish and removed > 90% of them in the final microcultures. To increase the number of microcultures established in the presence of Schwann cells, the duration of the preplate period was reduced to ~30 min. At the end of preplate, medium was centrifuged for 2 min at 2000 g. The pellet was then resuspended in 1 ml of high serum medium. The cell suspension was then forcibly ejected 3 times through a hypodermic needle (25 gauge, 0.5 × 16 mm) to break up possible clusters of neurons. Neurons were plated on freshly sprayed collagen dots at a low density (2000–3000 cells ml<sup>-1</sup>) in plating medium. The composition of the plating medium was DMEM–F12 (1 : 1) containing 2.5% FBS, 2.5% rat serum (prepared in the animal care facility of the University of Barcelona), and 500 nM NGF (Alomone Laboratories, Jerusalem, Israel). To achieve a cholinergic phenotype, 2 nM ciliary neurotrophic factor (CNTF; Alomone Laboratories) was added to plating medium 2 or 3 days after culture preparation (Saadat *et al.* 1989). Culture medium was changed two or three times a week by removing half of the well volume.

### Current-clamp and voltage-clamp recordings

All experiments were performed in the whole-cell configuration using neurons microcultured for 10–15 days *in vitro*. Typical pipette resistances were 2–4 MΩ when filled with internal solution. Composition of the internal solution was (in mM): 130 potassium gluconate, 4 MgCl<sub>2</sub>, 0.02 BAPTA, 10 Hepes, 3 Na<sub>2</sub>ATP, 1 NaGTP, pH 7.2, 290 mosmol kg<sup>-1</sup>. External solution contained (in mM): 130 NaCl, 5 KCl, 2 MgCl<sub>2</sub>, 10 Hepes-hemisodium salt and 10 glucose, pH 7.4. The final CaCl<sub>2</sub> concentration was achieved by dilution from a 1 M stock solution (Sigma-Aldrich). All salts were from Sigma-Aldrich.

Before the addition of glucose and  $\text{CaCl}_2$ , the osmolality of the external solution was  $290 \text{ mosmol kg}^{-1}$ . For current clamp recordings potassium gluconate was replaced by KCl. Hexamethonium (Sigma-Aldrich) was prepared at  $100 \mu\text{M}$  in extracellular solution. The recombinant light chain of tetanus toxin was prepared and stored at  $-80^\circ\text{C}$ . Aliquots containing the catalytic domain of the toxin were only thawed once.

Current-clamp recordings were performed using an Axoclamp 2A amplifier (Molecular Devices, Union City, CA, USA). Voltage clamp experiments were carried out using an Axoptach-200B (Molecular Devices). Amplifiers were driven by an ITC-18 board (Instrutech, Great Neck NY, USA) using WCP software (Dr John Dempster, University of Strathclyde, [http://spider.science.strath.ac.uk/sipbs/page.php?page=software\\_ses](http://spider.science.strath.ac.uk/sipbs/page.php?page=software_ses)). Neurons were clamped at  $-60 \text{ mV}$  and stimulated by a  $1\text{--}2 \text{ ms}$  depolarization step that drove membrane potential to  $0 \text{ mV}$ . Autaptic currents were identified as inward currents that appeared immediately after the sodium current associated with the generation of an action potential (Bekkers & Stevens, 1991). Analysis was performed with custom made macros written in Igor Pro software 6.0 (Wavemetrics, Lake Oswego, OR, USA). All experiments were performed at room temperature ( $22\text{--}24^\circ\text{C}$ ).

### Immunocytochemistry

Cells were fixed with 4% paraformaldehyde for 30 min at room temperature. Blocking was performed for 2 h with 20% normal goat serum in a 0.2% Triton solution. All primary antibodies were incubated for 1 h at room temperature at the following dilutions: monoclonal VAMP-2 (Synaptic Systems, Göttingen, Germany) 1:1000; polyclonal synaptophysin (Synaptic Systems) 1:500; monoclonal S-100B (Abcam, Cambridge, UK) 1:1000; monoclonal fibronectin (Abcam) 1:100; polyclonal PSD-93 (or chapsyn-110, Chemicon) 1:1000; and monoclonal VAChT (NeuroMab, Davis, CA, USA) 1:500. Secondary antibodies labelled with Alexa dyes (Invitrogen) were used at 1:500 dilution and incubated at room temperature for 2 h. Synapse quantification was performed using Image J software from images obtained of neurons co-stained with VAMP-2 and PSD-93. An axo-somatic synapse was considered when there was a co-staining of the two markers in round structures  $0.5\text{--}1 \mu\text{m}$  in diameter, located in the periphery of the soma, which spanned two to three confocal sections ( $\sim 0.4 \mu\text{m}$  each). The proportion of non-neuronal cells stained for S-100B and fibronectin was calculated after staining nuclei with propidium iodide or to-pro-3 (Invitrogen).

## Results

### Microcultures of superior cervical ganglion neurons established functional cholinergic autapses

In the absence of glial cells or their secreted factors a single SCG neuron was able to successfully develop axon-like and dendrite-like processes circumscribed to a microdot of collagen, which we termed a single cell microculture (Fig. 1A). Growth of the dendritic tree was obvious during the first week in culture and during the second and third week numerous branches and ramifications became more common, similar to what has already been described (Furshpan *et al.* 1986b). The appearance of neurons developed together with non-neuronal cells was very similar to single-cell microcultures (Fig. 1B). The absence of supporting cells did not affect the formation of synapses because the presence of potential autapses along the dendritic network was demonstrated by the positive staining for VAMP-2 (Fig. 1C) and synaptophysin (Fig. 1D) in single cell microcultures (see also Fig. 2 for synapse quantification). In the SCG *in vivo*, preganglionic fibres tend to establish more axo-dendritic rather than axo-somatic synapses (Forehand, 1985). Similarly, single cell microcultures displayed a larger number of axo-dendritic autapses along their dendritic-like tree compared to the soma (Fig. 1C and D).

The works of Furshpan and coworkers demonstrated that SCG neurons are able to change their phenotype from adrenergic to cholinergic in defined culture conditions. Several factors can induce such change, for example, presence of a feeder layer of myocardiocytes, rat serum or growth factors (Furshpan *et al.* 1986b). In the present experimental conditions a cholinergic phenotype was induced by CNTF (Saadat *et al.* 1989). The location of putative cholinergic terminals was demonstrated by staining for the vesicular transporter of acetylcholine (Fig. 1E). Similarly to VAMP-2 and synaptophysin staining, the periphery of the collagen microdot showed a more marked presence of cholinergic terminals if compared to the somatic region. However, the contribution of these peripheral autapses was probably not reflected in electrophysiological recordings due to space-clamp limitations. Only those synapses located in the soma or nearby dendritic tree were likely to provide information (Fig. 1F).

The average resting membrane potential of SCG neurons grown in single cell microcultures was  $-51 \text{ mV}$  ( $n = 7$ ). After  $0.6\text{--}1 \text{ nA}$  current injections, neurons fired action potentials at frequencies ranging from 0.1 to 20 Hz. The nature of synaptic transmission was studied in experiments such as those depicted in Fig. 1G. Functional cholinergic autapses were revealed by twice challenging neurotransmission: first by hexamethonium, a specific blocker of ganglionic nicotinic receptors, and

second by removing calcium from the extracellular medium. Both manoeuvres suppressed autaptic EPSPs reversibly, thus demonstrating the presence of nicotinic autapses. Although SCG neurons in microculture may synthesize other neurotransmitters than acetylcholine (Furshpan *et al.* 1986a), a complete block of neurotransmission by hexamethonium was always achieved ( $n = 4$ ). Cholinergic synapses were therefore predominant under our experimental conditions.

What was the nature of non-neuronal cells present in the microcultures? In the superior cervical ganglion, Schwann cells are the most abundant non-neuronal cell type and display a slow growth in culture compared to fibroblasts originating from the perineurium (Freschi, 1982). The SCG also contains satellite cells and small intensely fluorescent (SIF) cells (Baluk, 1995). Although all these cell types could be potentially present in

a microculture, the morphology under the phase contrast microscope after 10 days *in vitro* supported a predominant Schwann cell population. This observation was confirmed by the fact that positive staining for the calcium binding protein S-100B was found in 97% of the non-neuronal cells present in the microcultures (1741 cells evaluated). Typically, all non-neuronal cells observed in a microculture expressed S-100B but this marker was absent from neurons (Fig. 2A). Previous immunohistochemical studies revealed the S-100B marker stains Schwann cells and satellite cells of the superior cervical ganglion (Cocchia & Michetti, 1981) and in addition, transgenic mice expressing fluorescent proteins under the control of the human S-100B promoter show a few Schwann cells enveloping a single postsynaptic neuron (McCann & Lichtman, 2008). On these bases the term 'Schwann cell' used in the present study refers

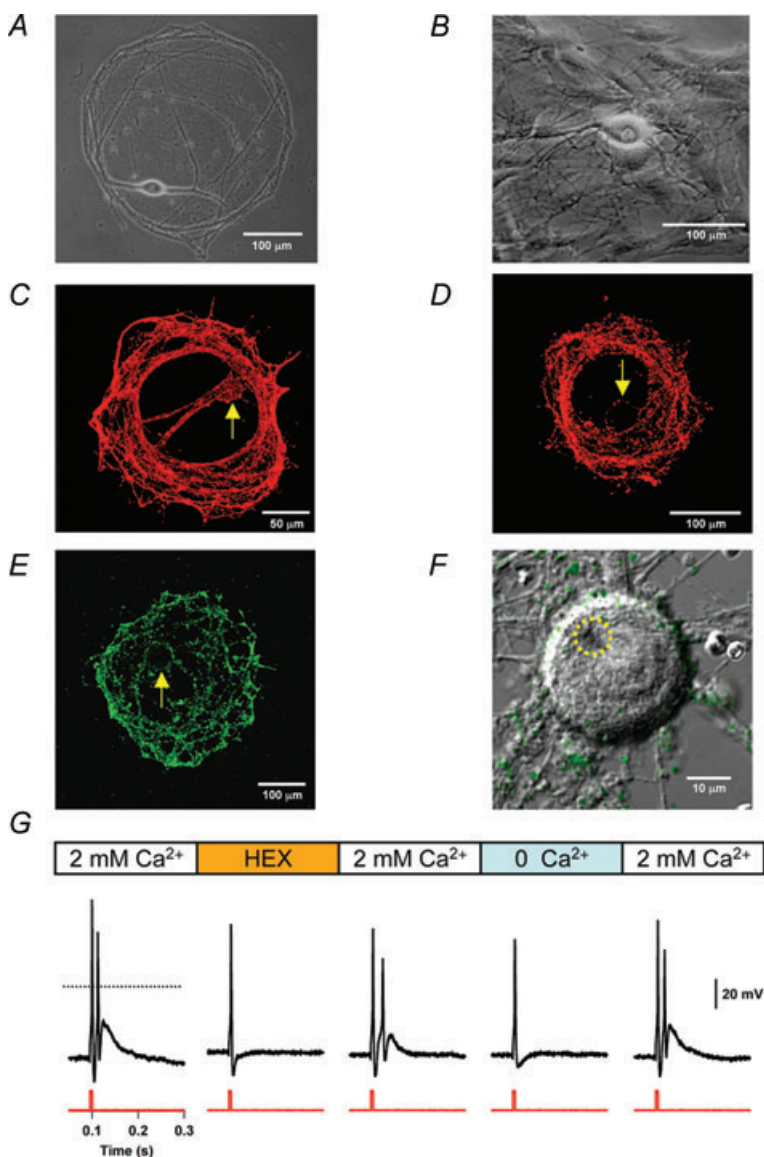


**Figure 1. Single cell microcultures of superior cervical ganglion neurons**

*A*, phase contrast image of a single cell microculture of a superior cervical ganglion neuron after 15 days *in vitro*. *B*, phase contrast image of a superior cervical ganglion neuron developed together with non-neuronal cells in a microculture, 12 days *in vitro*. *C–E*, single cell microcultures stained for VAMP-2, synaptophysin and vesicular acetylcholine transporter (vAChT), respectively. Arrows indicate the location of the soma. *F*, overlay of DIC and fluorescence images of the neuron shown in *E*. The neuron was patched and subsequently fixed and stained for vAChT. The circle with the dotted line indicates the location where the patch pipette was placed. *G*, representative current clamp experiment showing that autaptic responses were sensitive to hexamethonium (HEX) application and extracellular calcium removal. Note that both manoeuvres were reversible.

to S-100B immunoreactive glial cells, thus considering satellite cells as a type of Schwann cell (Mathey & Armati, 2007). Some glial cells tended to cluster around somas (Fig. 2A, arrows), whilst there were others associated with neuritic processes, further suggesting the presence of a heterogeneous Schwann cell population. The contribution of fibroblasts to the non-neuronal cell population was negligible, as revealed by fibronectin staining (Rohrer & Sommer, 1983). Only a few fibroblast clusters, which did not form part of the microcultures, were observed at the edges of coverslips (data not shown). Thus, microcultures containing non-neuronal cells were reproducing *in vitro* the interactions between Schwann cells and superior cervical ganglion neurons.

In order to evaluate the influence of glial cells on synaptogenesis, microcultures were co-stained with the postsynaptic and presynaptic markers, PSD-93 and VAMP-2, respectively (see Methods for details). As shown in Fig. 2B, axo-somatic synapses were rare after a few days in culture but showed a marked increase when neurons reached 10–15 days *in vitro*. Development of SCG neurons in culture is associated with an increase of their somatic surface (Johnson *et al.* 1980; see also Fig. 2A). Immediately after plating, neuron size was  $\sim 10 \mu\text{m}$ , and after 2 weeks in culture neurons of single cell microcultures increased their surface diameter to  $24 \pm 2 \mu\text{m}$  (mean  $\pm$  S.E.M.,  $n = 16$ ). Neurons developed in the presence of Schwann cells showed a similar growth to a size of  $26 \pm 2 \mu\text{m}$  (mean  $\pm$  S.E.M.,  $n = 16$ ). On these bases, the density of axo-somatic contacts was comparable in single cells and microcultures developed in a glial environment (Fig. 2C). Altogether, these results showed that Schwann cells neither promoted an increase of somatic surface nor enhanced the number of axo-somatic synapses. Axo-dendritic synapses were not evaluated because: (i) the complexity of the dendritic-like tree was very variable among microcultures, (ii) axo-dendritic synapses tended to form clusters, and (iii) most of the axo-dendritic synapses did not contribute to electrophysiological responses due to space clamp limitations.

To evoke synaptic transmission, the soma of a single microcultured SCG neuron was depolarized during 2 ms from a holding voltage of  $-60 \text{ mV}$  to  $0 \text{ mV}$ . In  $2 \text{ mM}$  extracellular calcium concentration ( $[\text{Ca}^{2+}]_o$ ) autaptic responses ranging from  $0.4$  to  $4 \text{ nA}$  were observed immediately after the sodium current peaked (Fig. 2D). The nature of evoked EPSCs was nicotinic because addition of  $100 \mu\text{M}$  hexamethonium at the end of the experiment always abolished them ( $n = 6$ , data not shown). In agreement with synaptic immunostainings, autaptic currents were never observed in microcultures developed for less than 10 days *in vitro*. In those cultures the sodium current was not followed by an autaptic response (Fig. 2D), showing a lack of mature cholinergic synapses.

### Spontaneous miniature EPSCs in microcultures established in the presence and absence of Schwann cells

Changing extracellular calcium concentration is a well established method to modify the release probability of synaptic terminals (Dodge & Rahamimoff, 1967). However, this manoeuvre could also have an effect at the postsynaptic level because SCG neurons express nicotinic receptors highly permeable to calcium (Trouslard *et al.* 1993). To investigate this possibility, the effect of  $[\text{Ca}^{2+}]_o$  on spontaneous miniature EPSCs (mEPSCs) was analysed by exposing neurons to  $1 \text{ mM}$ ,  $2 \text{ mM}$  and  $4 \text{ mM}$   $[\text{Ca}^{2+}]_o$  (Fig. 3).

The size of mEPSCs was variable, showing amplitudes ranging from  $20$  to  $140 \text{ pA}$  (Fig. 3A and B). Both, the intrinsic variability of postsynaptic responses and cable filtering properties of dendrite-like processes were likely to contribute to this wide distribution (Bekkers & Stevens, 1996). On average, the amplitude of mEPSCs was little affected by raising  $[\text{Ca}^{2+}]_o$  from  $1 \text{ mM}$  to  $4 \text{ mM}$ , but their duration was increased at the higher  $[\text{Ca}^{2+}]_o$  tested. The decay phase of mEPSCs was well fitted by a single exponential whose time constant rose gradually from  $1 \text{ mM}$   $[\text{Ca}^{2+}]_o$  to  $4 \text{ mM}$   $[\text{Ca}^{2+}]_o$  (Fig. 3C). As a result, mEPSCs obtained in high  $[\text{Ca}^{2+}]_o$  carried more charges into the cell (Fig. 3D). Calculation of mEPSCs integrals was therefore influenced by  $[\text{Ca}^{2+}]_o$ , whilst measurement of their amplitudes was relatively insensitive (Fig. 3E).

To investigate whether the presence of Schwann cells in the microculture could modify neurotransmission in autaptic synapses we first analysed mEPSCs. In this type of microcultures, and as described for single-cell ones, the rise in  $[\text{Ca}^{2+}]_o$  increased the decay phase of mEPSCs (Fig. 4A and B). As a result, mEPSCs found at high  $[\text{Ca}^{2+}]_o$  carried more charges into the cell (Fig. 4C), thus reflecting the high permeability of nicotinic receptors to  $\text{Ca}^{2+}$ . In terms of amplitude, no differences existed between mEPSCs obtained in single cell microcultures and in cultures developed in the presence of Schwann cells (Fig. 4D). The analysis of mEPSCs obtained in  $2 \text{ mM}$   $[\text{Ca}^{2+}]_o$  showed that their temporal profile was not modified by the presence of glial cells. The rise time from 20% to 80% was  $1.5 \text{ ms}$  ( $n = 102$ ) and  $1.3 \text{ ms}$  ( $n = 101$ ) for single cell and glial microcultures, respectively. In addition, there was no obvious correlation between mEPSC amplitudes and their decay time constant in both culture conditions (Fig. 4E). Altogether, Fig. 4A–E shows that the individual characteristics of mEPSCs did not change in the presence of Schwann cells, but they appeared at a frequency almost an order of magnitude higher when neurons developed in the glial environment (Fig. 4F; compare to Fig. 3A). Schwann cells increased synaptic activity from  $\sim 0.2$  to  $\sim 1.5 \text{ mEPSCs s}^{-1}$ . Such

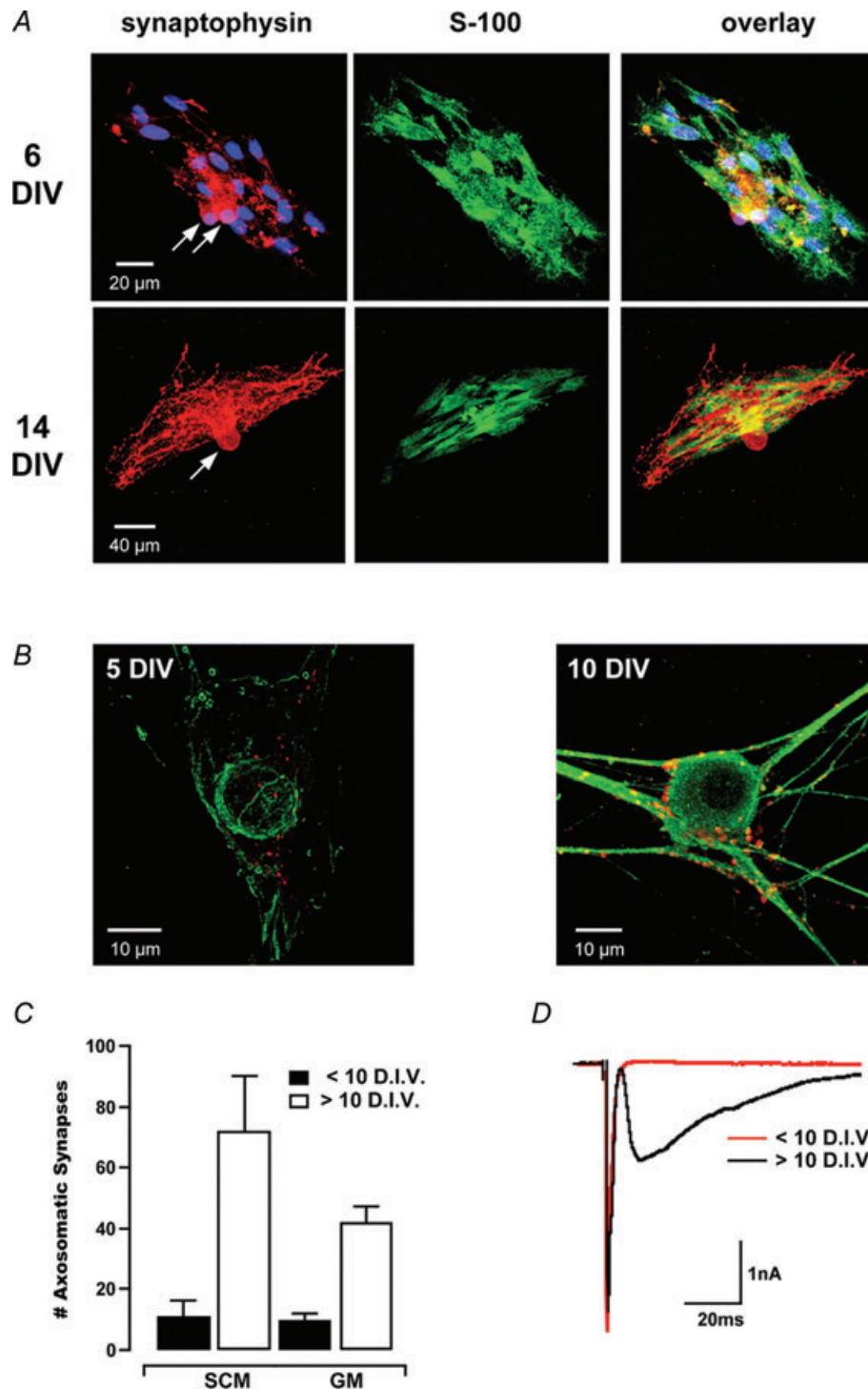
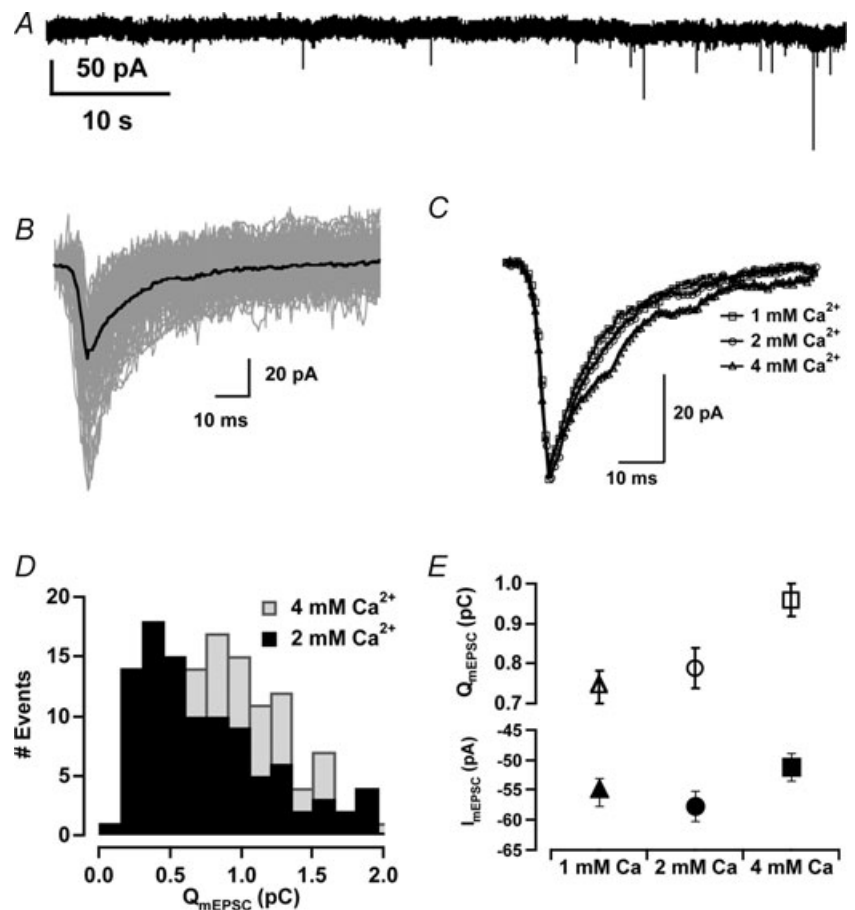


**Figure 2. Effect of glial cells on synaptogenesis**

*A*, images of two different microcultures co-stained for the presynaptic and glial cell markers synaptophysin and S-100B. The entire non-neuronal cell population was labelled with S-100B, a protein typically expressed in Schwann cells but not present in neurons. Arrows indicate the location of the somas. The upper microculture contained two neurons. Nuclei were labelled with to-pro-3, which are shown in blue. Note the increased soma size and the more complex neuritic tree in the older microculture. *B*, synaptogenesis was visualized by co-staining for the presynaptic and postsynaptic markers VAMP-2 (red) and PSD-93 (green), respectively. In single cell microcultures, synapses (yellow spots) were rare at 5 days *in vitro* (DIV) but covered the soma and dendritic-like process when the culture period extended further than 10 DIV. Only axo-somatic synapses were quantified (see Methods). *C*, summary of synaptogenesis observed in single cell and microcultures developed in the presence of glial cells, indicated as SCM

### Figure 3. Properties of spontaneous miniature excitatory postsynaptic currents in single cell microcultures

**A**, spontaneous miniature excitatory postsynaptic currents (mEPSCs) observed in a single cell microculture. Extracellular solution contained 1 mM  $\text{Ca}^{2+}$ . **B**, traces from 56 mEPSCs coming from 2 different neurons bathed in 2 mM  $\text{Ca}^{2+}$ . The average mEPSC for this set of recordings is shown in black. **C**, average mEPSCs for 1 mM  $[\text{Ca}^{2+}]_o$  ( $n = 50$ , 4 cells), 2 mM  $[\text{Ca}^{2+}]_o$  ( $n = 102$ , 5 cells) and 4 mM  $[\text{Ca}^{2+}]_o$  ( $n = 106$ , 3 cells). Single exponential fits showed that mEPSCs prolonged their duration when  $[\text{Ca}^{2+}]_o$  increased. Time constants were 11 ms, 13 ms and 18 ms for 1 mM, 2 mM and 4 mM  $[\text{Ca}^{2+}]_o$ , respectively. **D**, distribution of charges carried by mEPSCs in 2 mM and 4 mM  $[\text{Ca}^{2+}]_o$ . **E**, average values of amplitude and charge carried by mEPSCs as a function of  $[\text{Ca}^{2+}]_o$ . Note that the amplitude of mEPSCs showed little variation when  $[\text{Ca}^{2+}]_o$  changed in the range of 1 mM to 4 mM. Error bars indicate S.E.M.



enhancement of spontaneous neurotransmission was not associated with a larger number of active synapses because Schwann cells did not promote synaptogenesis of axo-somatic synapses (Fig. 2C). Hence, Schwann cells had a direct effect on the spontaneous activity of nicotinic autapses, but what was their effect on evoked neurotransmission?

### Neurotransmission in cholinergic autapses studied at low frequencies of stimulation

Long periods of recording allowed the diffusion of the intracellular solution from the patch pipette to neuritic processes. This phenomenon was seen by the addition of 0.2 mM tetramethyl-rhodamine labelled 3 kDa dextran to the internal solution. Staining of processes was obvious after 28 min of dialysis. Maximum dye accumulation was at dendrites located in the proximity of the soma

but labelling of  $\sim 1 \mu\text{m}$  diameter axon-like processes was also observed (see Supplementary Fig. 1). To test whether the presence of dye along the axon was reflecting a washout of synaptic proteins, rundown for autaptic responses was tested in recordings lasting more than 30 min ( $n = 6$ ). In this set of neurons series resistance was maintained around initial levels for more than 50 min. Although the amplitude of EPSCs was decreased by 25% at the end of the recording period, little rundown was observed in the charge carried by autaptic responses (Fig. 5). This observation confirmed that Schwann cells were not required for the robustness of the experimental preparation.

Long lasting recordings offered the possibility to investigate the effect of recombinant proteins able to interfere with presynaptic function. When the recombinant light chain of tetanus toxin was diluted to  $2 \mu\text{M}$  in the internal patch solution, it blocked

and GM, respectively. The presence of Schwann cells did not modify the number of axo-somatic synapses after 10 DIV. **D**, the black trace shows an evoked autaptic response by application of a 2 ms depolarization via a patch pipette placed at the soma. An initial inward current corresponding to the sodium current associated with the generation of an action potential was followed by a nicotinic EPSC. The red trace shows a typical response of a microculture lacking mature synapses, because only the sodium current is observed.

neurotransmission. Success, however, was only achieved in small microdots and it developed after  $\sim 25$  min of recording (Fig. 5). The molecular weight of the light chain of tetanus neurotoxin is 50 kDa, more than 10 times larger than the fluorescently labelled dextran used to evidence neuritic processes. This difference probably caused a slower diffusion through long, tortuous axon-like processes. Obtaining a successful delivery of recombinant proteins to presynaptic terminals therefore required the use of small microdots, usually not bigger than  $\sim 100 \mu\text{m}$  diameter.

Long lasting recordings where responses were evoked at stimulation frequencies ranging from 0.1 to 1 Hz did not show obvious plasticity features. On average, the amplitude of EPSCs showed little variation during the initial 20–25 min of recording. During this period,  $R_s$  showed little change, since it increased from an average value of  $14 \text{ M}\Omega$  to  $17 \text{ M}\Omega$  ( $n = 28$ ). However, only a few neurons were recorded after this time window, because significant increases of the initial series resistance developed.

### Synaptic plasticity of single cell microcultures evoked by high frequency stimulation

Experiments *in vivo* have shown that preganglionic fibres innervating the SCG ganglion fire at a maximal frequency of 10–40 Hz (Birks & Isacoff, 1988; Huang & Cohen, 2000). Trains of stimuli delivered at frequencies up to 20 Hz evoked action potentials without showing failures in SCG single cell microcultures (data not shown), and a frequency of 14 Hz was chosen to test for use-dependent plasticity mechanisms. Depression was consistently evoked when  $[\text{Ca}^{2+}]_o$  was above 1 mM but was absent below this concentration (Fig. 6A). The amplitude of autaptic responses in 0.5 mM and 2 mM  $[\text{Ca}^{2+}]_o$  was  $715 \pm 34 \text{ pA}$  ( $n = 5$ ) and  $1872 \pm 119 \text{ pA}$  ( $n = 12$ ), respectively, meaning that the release probability at which the synapse was operating was key to determining the presence of synaptic depression during high frequency stimulation.

In 2 mM  $[\text{Ca}^{2+}]_o$  depression reached a steady state value after four to six depolarizations delivered at 14 Hz

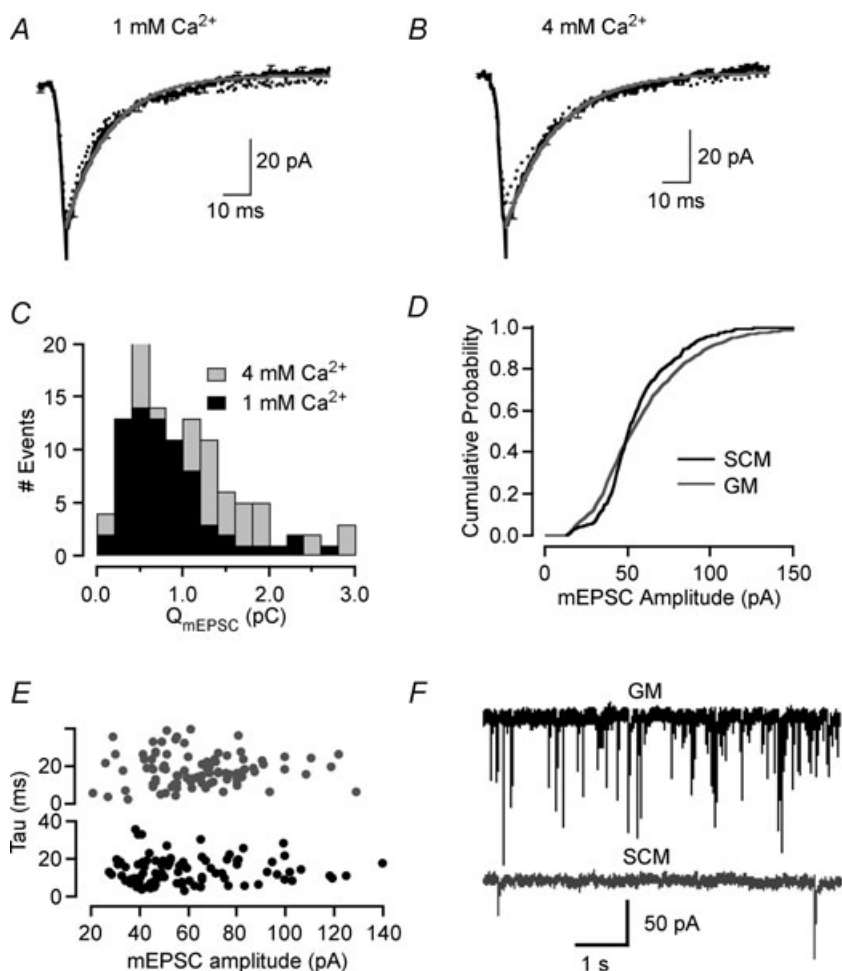


**Figure 4. Properties of spontaneous miniature excitatory postsynaptic currents in microcultures established in the presence of Schwann cells**

*A*, average mEPSC obtained in 1 mM  $[\text{Ca}^{2+}]_o$  ( $n = 67$ , 3 cells, black trace). Grey line indicates an exponential fit to the decay phase;  $\tau = 14$  ms. Dotted line indicates the average mEPSC from single cell microcultures in 1 mM  $[\text{Ca}^{2+}]_o$ . *B*, average mEPSC obtained in 4 mM  $[\text{Ca}^{2+}]_o$  ( $n = 89$ , 5 cells, black trace). Grey line indicates an exponential fit to the decay phase,  $\tau = 20$  ms. Dotted line indicates the average mEPSC from single cell microcultures in 4 mM  $[\text{Ca}^{2+}]_o$ . *C*, distribution of charges carried by mEPSCs in 1 mM and 4 mM  $[\text{Ca}^{2+}]_o$ .

*D*, cumulative probability plot of mEPSC amplitudes observed in single cell microcultures (SCM, 19 min recorded from 10 neurons,  $n = 495$ ) and microcultures developed in the presence of glia (GM, 41 min recorded from 5 neurons,  $n = 2789$ ). *E*, plot of mEPSC decay time constants against their amplitude for SCM (black) and GM (grey). *F*, recordings of spontaneous activity in SCM and GM. Note the enhanced mEPSC frequency in GM.

(Fig. 6A). By using cumulative plots of EPSC amplitudes it was possible to fit a line to the steady-state phase of synaptic depression and extrapolate it to time 0 (Fig. 6B). Assuming the refilling of the readily releasable pool of vesicles (RRP) took place uniformly throughout stimulation, the intercept on the Y-axis reported an estimate of the RRP size (see Supplementary Fig. 2 for details of the procedure). This type of calculation has been previously performed at the calyx of Held synapse (Schneppenburger *et al.* 1999), hippocampal synapses in microculture (Otsu *et al.* 2004) and neuromuscular junctions (Millar *et al.* 2002). The main constraint on performing this calculation was that it could only be applied if synaptic depression developed. Therefore, it was not a valid approach to establish the size of the RRP in conditions of low release probability, for example at 0.5 mM  $[Ca^{2+}]_o$  (Fig. 6A and B).

The RRP is heterogeneous among synapses and its definition greatly depends on the method used (Murthy *et al.* 1997). For example, the measurement of the RRP size by using a train of action potentials in hippocampal synapses reported different estimations from another well-established method, the application of a hypertonic sucrose solution (Rosenmund & Stevens, 1996; Moulder & Mennerick, 2005). We defined the RRP size using plots of cumulative EPSC amplitudes, so that it only took into consideration the contribution of vesicles released synchronously with stimulation. The participation of some vesicles from the RRP in asynchronous release has been recently revealed (Stevens & Williams, 2007). Their contribution can be taken into account by analysing EPSC charges instead of currents. This approach, however, was not performed. Nicotinic receptors displayed a high permeability to calcium, and changes in  $[Ca^{2+}]_o$  affected both the probability of release and the amount of charge carried by EPSCs (Figs 3 and 4). In contrast, the amplitude of mEPSCs was constant under variable  $[Ca^{2+}]_o$ . Hence, this parameter provided a measurement of the presynaptic effects of changes in  $[Ca^{2+}]_o$ , with little postsynaptic contribution.

Typically, in 4 mM  $[Ca^{2+}]_o$ , the RRP was exhausted at the fourth action potential of the train, while in 1 mM  $[Ca^{2+}]_o$ , at least six stimuli were required (Fig. 6C and D). Steady state depression was always achieved faster under high release probability conditions. In terms of the fraction of the RRP released by the first action potential of the train, a rise from 1 mM to 4 mM  $[Ca^{2+}]_o$  at most doubled the amount of vesicles mobilized (Fig. 6E). When  $[Ca^{2+}]_o$  was 1 mM, the arrival of an action potential released approximately a third of the RRP but in 4 mM  $[Ca^{2+}]_o$ , almost two-thirds were released. This change in the kinetics of depression, however, did not affect the total number of vesicles mobilized from the RRP. The average of seven different neurons successively trialled with 1 mM, 2 mM and 4 mM  $[Ca^{2+}]_o$  showed that the estimates for the RRP size were independent of release probability at which

synapses were operating (Fig. 6E). Remarkably, the size of the RRP was not modified in the presence of Schwann cells (Fig. 7A).

### Determinants of paired pulse plasticity in cholinergic autapses

Paired pulse stimuli are a simple approach to probe synaptic plasticity. Paired pulse facilitation (PPF) is defined by a paired pulse ratio (PPR) larger than 1, whilst paired pulse depression (PPD) is defined by a PPR < 1. The red and blue traces in the example of Fig. 6C show that a change from PPF in 1 mM  $[Ca^{2+}]_o$  to PPD in 4 mM  $[Ca^{2+}]_o$  took place if the two initial stimuli of the trains of action potentials were considered. As shown in Fig. 6E, in 1 mM  $[Ca^{2+}]_o$ , the first action potential of a train of stimuli released a variable range of vesicles, from 25% to 55% of the whole RRP, whilst in 4 mM  $[Ca^{2+}]_o$ , this range rose from 40% to 70%. The trains of action potentials were therefore used to define the relationship between the PPR for a 70 ms interval and the fraction of the RRP released by the first action potential of the train ( $R_f$ ) in single cell microcultures. An experimentally determined power function described the relationship:

$$PPR = 0.4/R_f^{0.94}$$

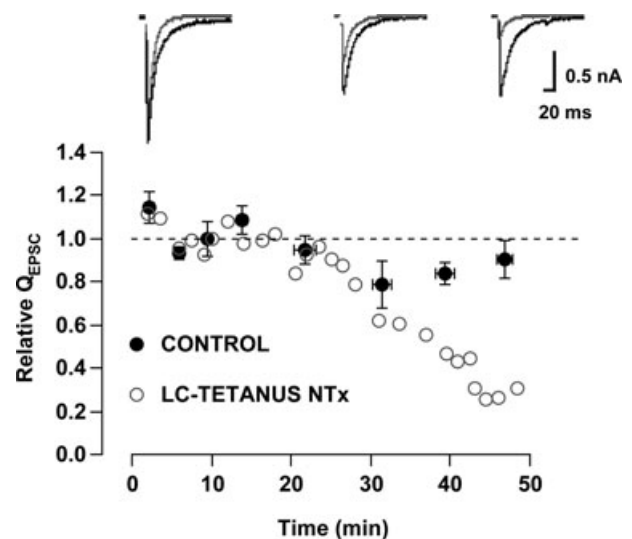


**Figure 5. Recordings of synaptic responses at low frequencies of stimulation**

Long-lasting recordings of autaptic activity. Traces show EPSCs obtained at the indicated times in a single neuron dialysed with standard internal solution (black). Sodium currents were cancelled for illustration purposes. EPSC charges displayed little rundown relative to the initial 10 min of recording ( $n = 6$ ). When pipette solution contained 2  $\mu$ M light chain of tetanus neurotoxin there was an obvious decay of the response after ~30 min of recording (red). Error bars indicate S.E.M.

In general terms, it could be considered that  $R_f$  was inversely related to PPR (Fig. 7B, open symbols). The relationship between PPR and  $R_f$  in microcultures developed in the presence of Schwann cells also followed

well the above function (Fig. 7B, dots). The analysis of trains of stimuli also allowed the study of whether (i) there was a relation between PPR and the RRP size and (ii) PPR was affected by postsynaptic mechanisms.

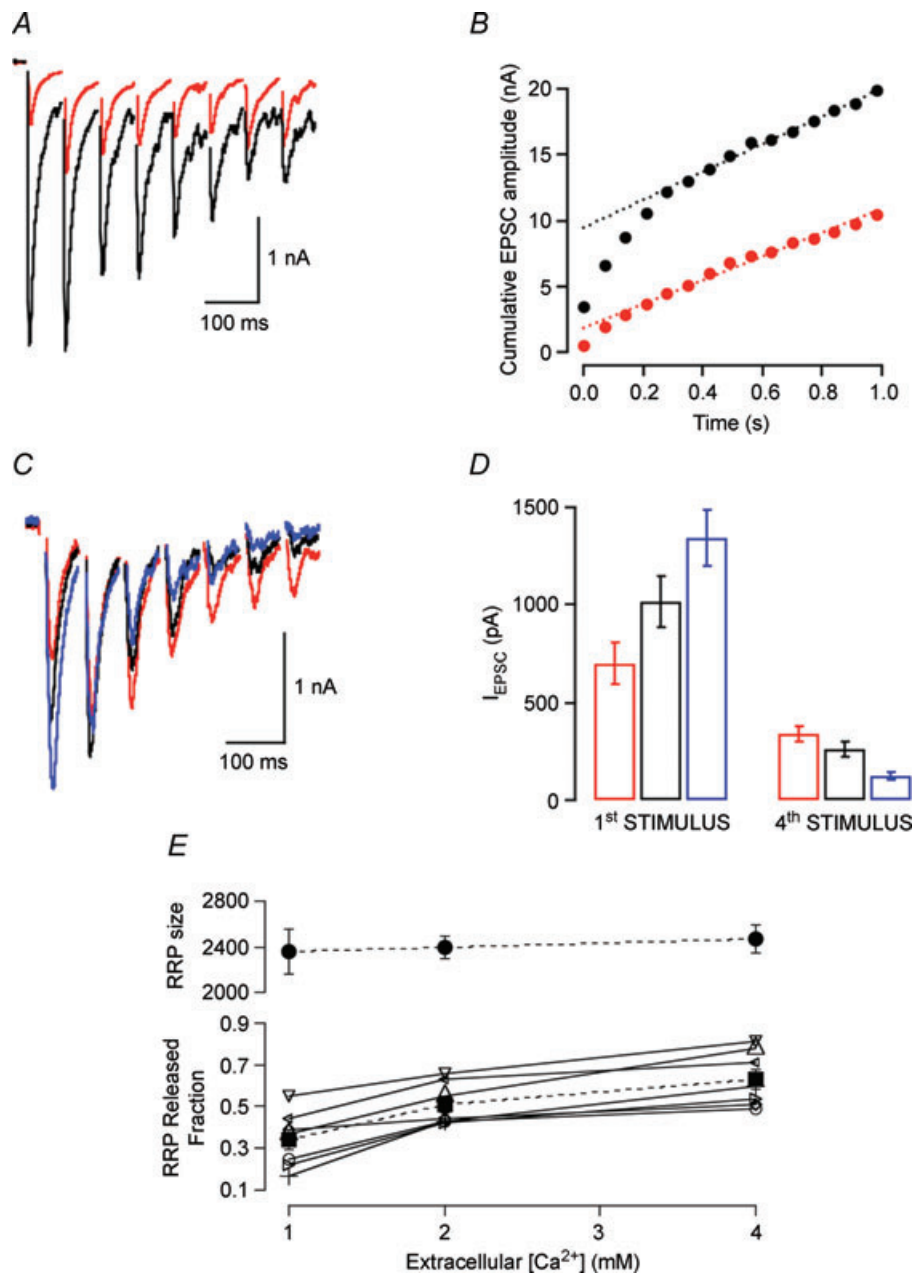


**Figure 6. High frequency stimulation evoked short-term depression**

A, EPSCs evoked by a train of stimuli delivered at 14 Hz in 0.5 mM [Ca<sup>2+</sup>]<sub>o</sub> (red) and 2 mM [Ca<sup>2+</sup>]<sub>o</sub> (black) in a single cell. Depression was obvious in 2 mM [Ca<sup>2+</sup>]<sub>o</sub>. B, cumulative plots of EPSC amplitudes obtained from the traces shown in A. A linear function was fitted to the steady-state phase of depression (dotted line). The Y-axis intercept provided an estimate of the readily releasable pool (RRP) size (see text). C, EPSCs evoked by a train of stimuli in a cell successively exposed to 1 mM [Ca<sup>2+</sup>]<sub>o</sub> (red), 2 mM [Ca<sup>2+</sup>]<sub>o</sub> (black) and 4 mM [Ca<sup>2+</sup>]<sub>o</sub> (blue). Note the differences in amplitude of the first response of the train in the three experimental conditions tested. D, average EPSC amplitude for the first and fourth stimulus of the train in 7 cells exposed to three different [Ca<sup>2+</sup>]<sub>o</sub>: 1 mM (red), 2 mM (black) and 4 mM (blue). E, the upper left axis plots the size of the RRP estimated with the method described in B as a function of [Ca<sup>2+</sup>]<sub>o</sub>, and the lower left axis shows the fraction of the RRP released by the first action potential of the train, both as a function of [Ca<sup>2+</sup>]<sub>o</sub>. Open symbols indicate individual values and filled squares indicate means  $\pm$  s.e.m. Data come from 7 cells sequentially exposed to 1 mM, 2 mM and 4 mM [Ca<sup>2+</sup>]<sub>o</sub>.

A direct relation between PPR and the average RRP size was not found in single cell microcultures, this meaning that the number of vesicles available for release was unrelated to short-term plasticity phenomena (Fig. 7C). Microcultures developed in the presence of Schwann cells also did not show an obvious relationship (Fig. 7D).

Saturation of postsynaptic receptors can induce a process of short-term depression (Zucker & Regehr, 2002). Hence, there was the possibility that the size of postsynaptic responses was related to the type of plasticity displayed, i.e. the larger EPSCs were associated with a more marked depression. As depicted in Fig. 7E, there was not an

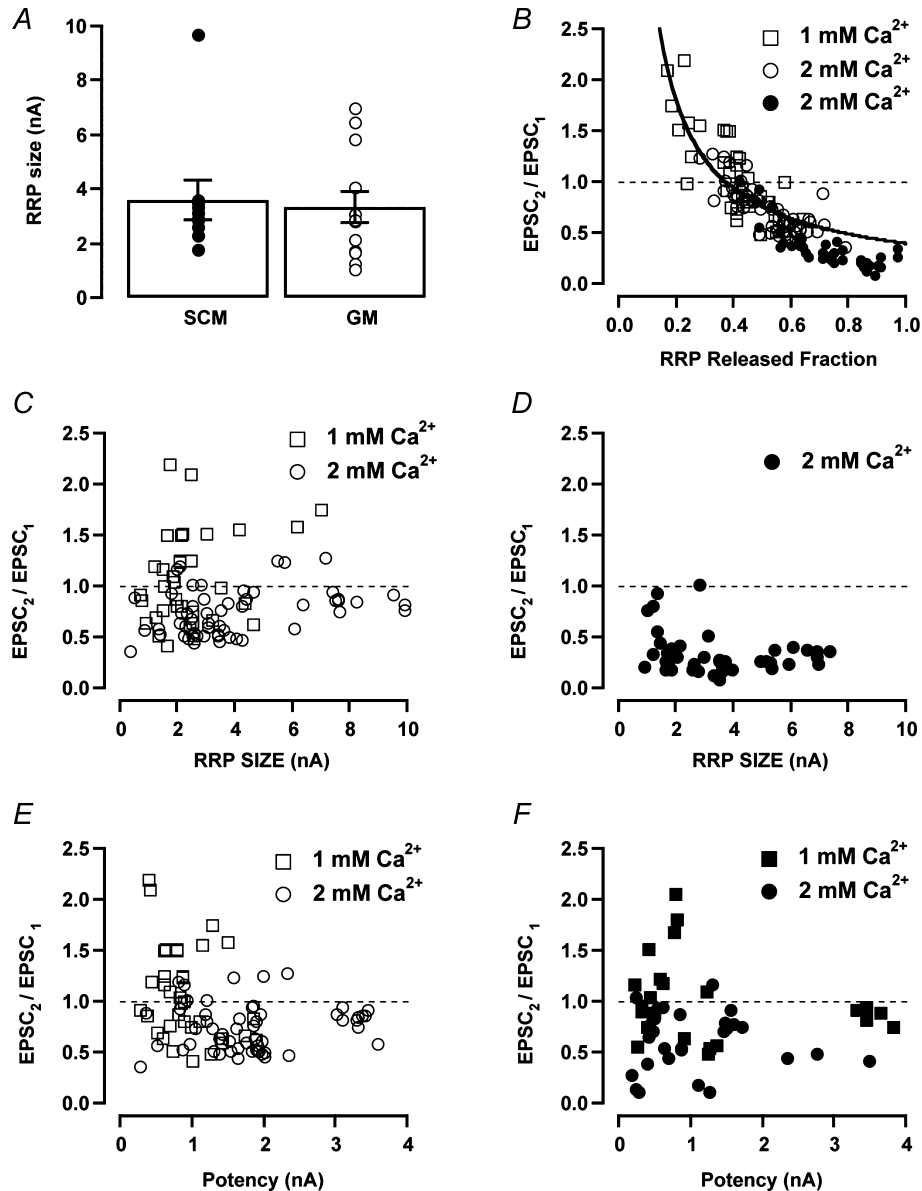


**Figure 7. Relationship of paired pulse ratio with presynaptic and postsynaptic parameters**

A, summary of the readily releasable pool (RRP) sizes obtained in single cell microcultures (SCM) and microcultures developed in the presence of glial cells (GM). B–F, the two initial stimuli of a train of depolarizations were used to calculate the paired pulse ratio (PPR) for a 70 ms interval. The results obtained were plotted against parameters related to presynaptic or postsynaptic function. Graphs illustrate results obtained in single cell microcultures (open symbols) and in microcultures developed in the presence of Schwann cells (filled symbols). B, plot of PPR against the fraction of vesicles released from the readily releasable pool (RRP) by the first action potential of the train. The size of the RRP was calculated following the method described in Fig. 6B. Points obtained for SCM were well fitted by a power function (straight line, see text). C and D, plot of the paired pulse ratio against the size of the readily releasable pool in SCM and GM. E and F, plot of PPR against the amplitude of the first EPSC of the train (synaptic potency) in SCM and GM. The size of postsynaptic currents was unrelated to PPR in both types of microcultures tested.

obvious relation between PPR and synaptic potency, measured as the amplitude of the first EPSC of the train. Thus, the observed changes in PPR in single cell microcultures were essentially of presynaptic origin. A similar result was obtained in microcultures developed in the presence of Schwann cells (Fig. 7F).

### Effect of Schwann cells on the short-term plasticity displayed by cholinergic autapses

Schwann cells did not modify the RRP size (Fig. 7A), but instead altered PPR in conditions of high release probability. Comparison between Fig. 7C and D illustrates this observation. PPR was decreased in glial microcultures but the RRP size was unaffected. To further investigate this aspect, paired pulse stimuli were applied in successive trials in single cell microcultures (Fig. 8A) and compared to neurons microcultured in the presence of glial cells (Fig. 8B). As expected (Figs 6 and 7), PPD was consistently evoked when  $[Ca^{2+}]_o$  was above 2 mM and pulse intervals were shorter than 0.5 s (Fig. 8C). However, neuronal development together with Schwann cells significantly affected depression. In this condition, PPD was longer lasting and was still present at a 1 s interval (Fig. 8D). When the  $[Ca^{2+}]_o$  of the bathing medium was lowered to 0.5 mM, neurons changed PPD to PPF. Facilitation was obvious for pulse intervals up to 100 ms and was comparable between the two types of microcultures (Fig. 8E and F). The time course of PPF was exponential and showed a time constant of  $\sim 0.5$  s in both cases (Fig. 8G and H). The temporal profile of PPD was also exponential but about 10 times faster than PPF. This observation, however, was valid only in single cell microcultures because Schwann cells prolonged the process of depression. In this condition the time course of PPD was comparable to PPF (Fig. 8H).

Paired pulse depression was evoked in single cell microcultures when  $[Ca^{2+}]_o$  was both 2 mM (Fig. 9A) and 4 mM (Fig. 9B). In this type of culture the time course of PPD followed time constants of 41 ms and 83 ms in 2 mM and 4 mM  $[Ca^{2+}]_o$ , respectively (Fig. 9A and B, right). On average, the presence of Schwann cells significantly slowed down recovery from depression. In this condition, the process became bi-exponential (Fig. 9A and B, grey traces). In 2 mM  $[Ca^{2+}]_o$  PPD took place with fast and slow time constants of 14 ms and 2 s, respectively, while in 4 mM  $[Ca^{2+}]_o$  this process was even slower, providing time constants of 0.4 s and 31 s. Therefore, Schwann cells were modulating the degree of short-term depression. In addition to the fact that short-term plasticity phenomena are considered essentially presynaptic processes (Zucker & Regehr, 2002), three pieces of experimental evidence favoured a specific effect of Schwann cells at the presynaptic level: (i) synaptic potency was not significantly affected by the presence of glial cells (Fig. 9A and B, left,

see also Fig. 10), (ii) PPR was unrelated to the amplitude of the first EPSC (Fig. 7E and F), and (iii) mEPSCs, which reflect basic properties of postsynaptic nicotinic receptors, did not change their characteristics in the presence of glial cells. As a result, it was concluded that Schwann cells were enhancing the short-term depression displayed by cholinergic autapses by acting at the presynaptic level.

Decrease of  $[Ca^{2+}]_o$  below 2 mM  $[Ca^{2+}]_o$  shifted the tendency of paired pulse stimuli to evoke depression. For example, for a 100 ms interval, in 4 mM  $[Ca^{2+}]_o$  all cells tested evoked PPD, in 2 mM  $[Ca^{2+}]_o$  the proportion was reduced to 90% of the neurons and in 1 mM  $[Ca^{2+}]_o$  only 5 out of 10 single cell microcultures displayed depression (Figs 9 and 10, left). Nevertheless, the net effect in 1 mM  $[Ca^{2+}]_o$  was PPF (Fig. 10A), this meaning that the degree of facilitation was larger than depression in this condition. When neurons were bathed in 0.5 mM  $[Ca^{2+}]_o$ , only facilitation was evoked (Fig. 10B). PPF followed an exponential time course and was longer lasting in 0.5 mM  $[Ca^{2+}]_o$  ( $\tau = 0.8$  s) than in 1 mM  $[Ca^{2+}]_o$  ( $\tau = 0.41$  s). In contrast to the results found for depression, microcultures developed in the presence of Schwann cells showed a comparable facilitation time course to single cell microcultures (Fig. 10), providing time constants of 0.72 s and 0.28 s in 0.5 mM and 1 mM  $[Ca^{2+}]_o$ , respectively. The longest time constants were thus associated with the lowest release probability condition tested, where fewer vesicles were mobilized from the RRP (Fig. 6E). Altogether, the present results support a scenario where autapses switch between PPF and PPD within a continuous process, which is inversely proportional to release probability. Schwann cells exert a specific effect on synaptic plasticity, enhancing short-term depression but having no effect on facilitation.

## Discussion

Although perisynaptic Schwann cells modulate synaptic depression during a train of stimuli at the neuromuscular junction (Robitaille, 1998), it is still unknown whether other peripheral synapses covered by glial cells display comparable phenomena. The present data show that Schwann cells exert a very well defined action on synaptic plasticity of cholinergic autapses by modulating their degree of depression but without modifying the number of synapses established or affecting facilitation.

Schwann cells have the general property of promoting synaptogenesis (Ullian *et al.* 2004), but the density of axo-somatic synapses was similar between single cell and glial microcultures. This result was supported by the fact that the amplitude of EPSCs generated both in single cell and glial microcultures was comparable. The concentration of NGF was a key factor in obtaining

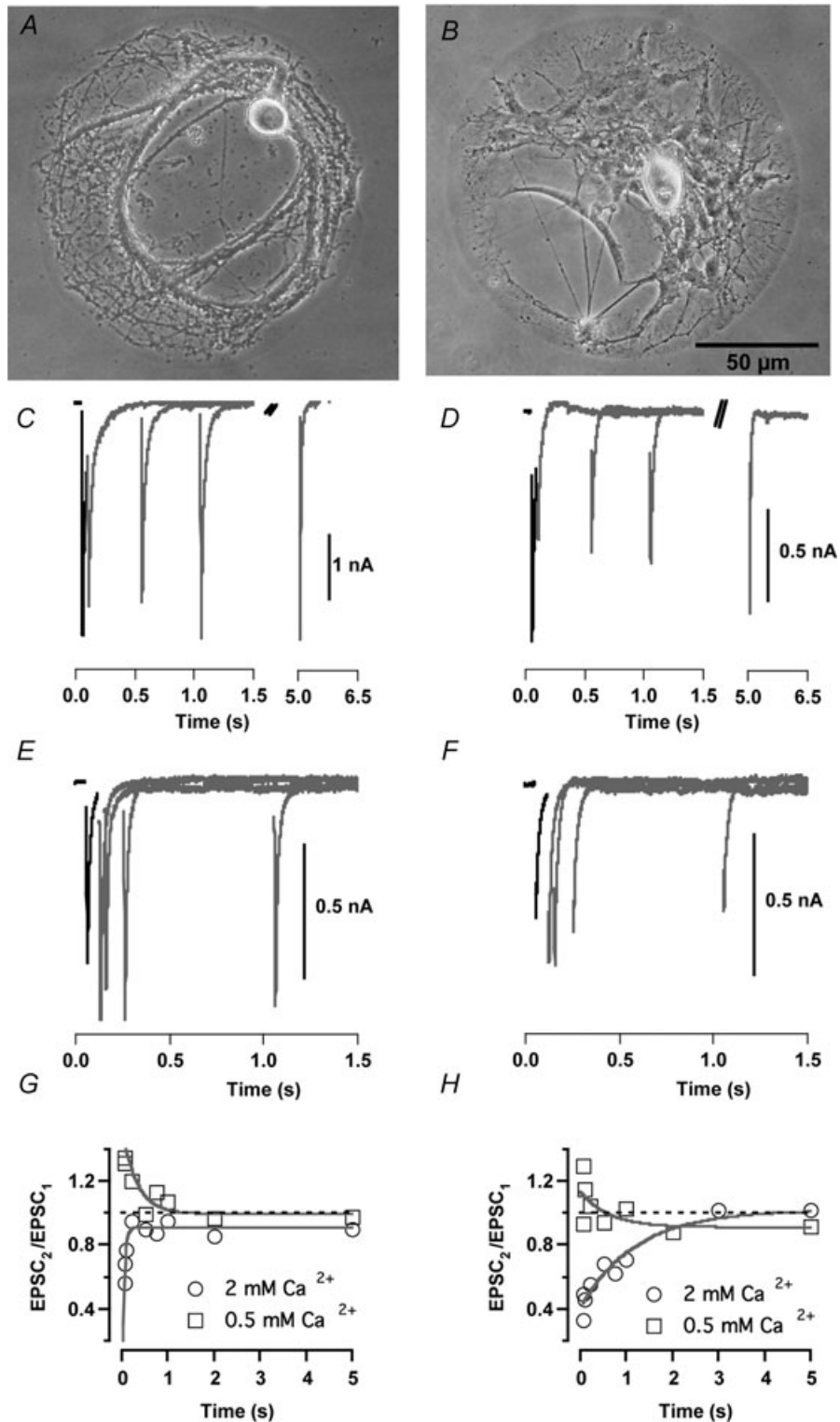


**Figure 8. Paired pulse ratio in single cell microcultures and microcultures developed with Schwann cells**  
*A*, phase contrast image of a single cell microculture before patching. *B*, image of a microculture developed in the presence of non-neuronal cells after withdrawing the recording electrode. *C* and *D*, paired pulse depression evoked in 2 mM  $[Ca^{2+}]_o$  on neurons shown in *A* and *B*, respectively. The average first EPSC of the series is shown in black. Second EPSCs obtained at several time intervals are shown in grey. Note the different degree in paired pulse depression between *C* and *D*. *E* and *F*, paired pulse facilitation evoked in 0.5 mM  $[Ca^{2+}]_o$  on neurons shown in *A* and *B*, respectively. *G* and *H*, time courses of recovery from depression and facilitation for neurons shown in *A* and *B*, respectively. Grey lines indicate single exponential fits.

successful microcultures. Autapses were only achieved using concentrations of NGF above  $500 \text{ ng ml}^{-1}$ , similarly to previously reported values (Furshpan *et al.* 1986b). In contrast, a concentration of  $25 \text{ ng ml}^{-1}$  is enough to establish cholinergic synapses in mass cultures of SCG neurons containing non-neuronal cells (Mochida *et al.* 1994). The different NGF requirements might be attributed to the fact that some non-neuronal cells, such as fibroblasts (Oger *et al.* 1974) and particularly Schwann cells, have the ability to synthesize and secrete a wide range of growth factors, NGF being one of them (Assouline *et al.* 1987; Bampton & Taylor, 2005).

Development and synaptogenesis of the SCG requires NGF (Crowley *et al.* 1994), which mediates its action in a concentration-dependent manner (Chun & Patterson, 1977). It is thus possible that the high NGF concentration used in the study masked the synaptogenic effect of Schwann cells, but remarkably, synapses grown in direct contact with a glial environment showed a different activity from those established in single cell microcultures. They displayed two distinctive features: an enhanced frequency of mEPSCs and a longer period to recover from short-term depression.

Short-term depression can be explained by a depletion of vesicles from the RRP that occurs at high release probabilities during repetitive stimulation (Zucker &

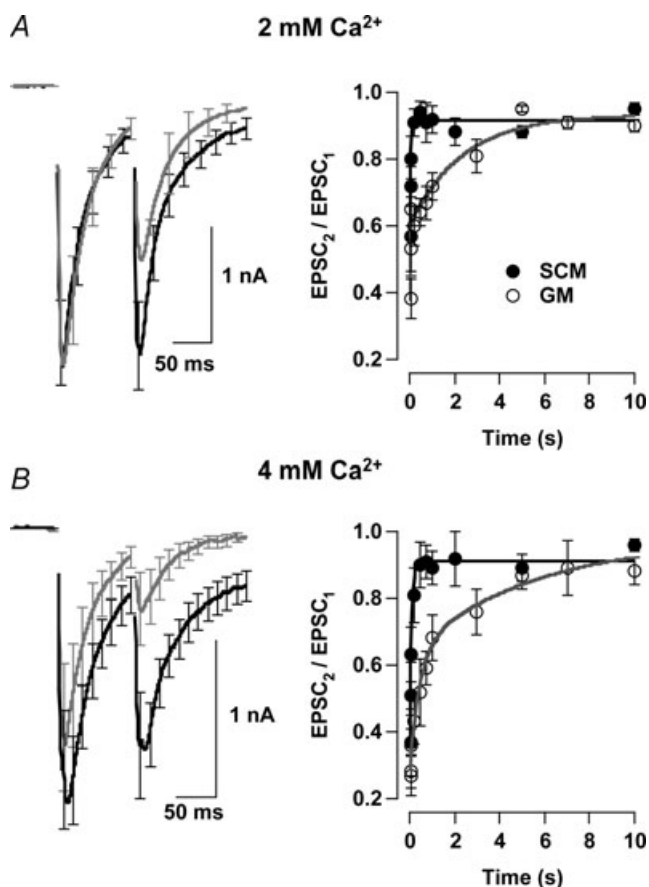


#### Figure 9. Schwann cells modified paired pulse depression

Paired pulse depression (PPD) was studied at  $2 \text{ mM } [\text{Ca}^{2+}]_o$  and  $4 \text{ mM } [\text{Ca}^{2+}]_o$ . *A*, left, traces showing the average EPSCs obtained for a pulse interval of  $100 \text{ ms}$  in  $2 \text{ mM } [\text{Ca}^{2+}]_o$ . Single cell microcultures (SCM, black,  $n = 12$ ) and microcultures developed in the presence of glial cells (GM, grey,  $n = 11$ ). Right, recovery from depression illustrated as paired pulse ratio plotted against time. SCM showed a PPD that recovered exponentially ( $\tau = 41 \text{ ms}$ ), while GM recovered more slowly, following a double exponential, providing fast and slow time constants of  $14 \text{ ms}$  and  $2 \text{ s}$ , respectively. *B*, left, PPD was enhanced both in SCM ( $n = 10$ ) and GM ( $n = 9$ ) by raising  $[\text{Ca}^{2+}]_o$  to  $4 \text{ mM}$ . In this condition, PPD recovered exponentially in SCM;  $\tau = 83 \text{ ms}$ . Again, in the presence of non-neuronal cells, recovery from PPD was best fitted with a double exponential ( $\tau_1 = 0.4 \text{ s}$  and  $\tau_2 = 31 \text{ s}$ ). Error bars indicate s.e.m. Each point shows the average of values obtained in  $\geq 6$  different cells.

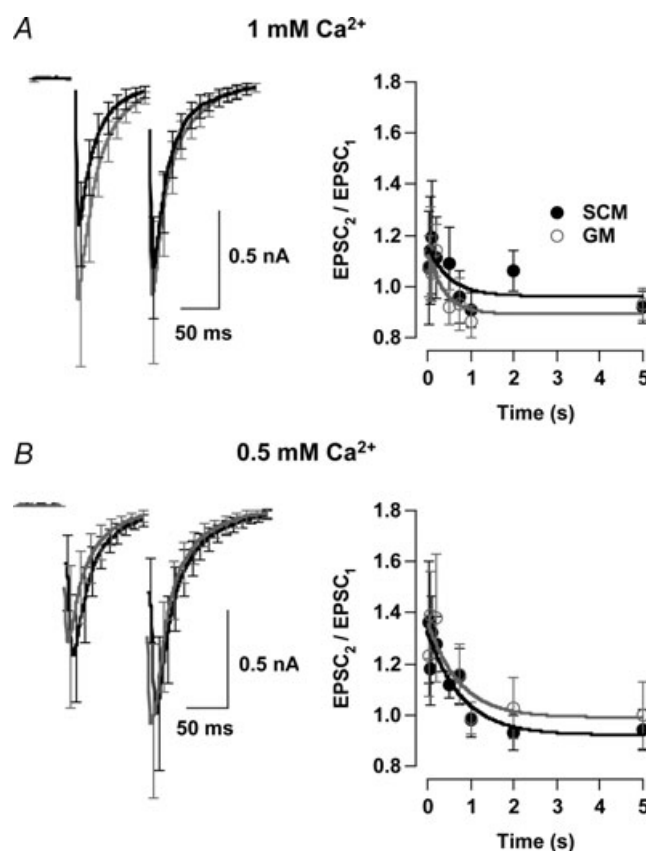


#### Figure 10. Schwann cells did not modify paired pulse facilitation

Paired pulse facilitation (PPF) was studied at  $1 \text{ mM } [\text{Ca}^{2+}]_o$  and  $0.5 \text{ mM } [\text{Ca}^{2+}]_o$ . *A*, left, traces showing the average EPSCs obtained for a pulse interval of  $100 \text{ ms}$  in  $1 \text{ mM } [\text{Ca}^{2+}]_o$ . Single cell microcultures (SCM, black,  $n = 10$ ) and microcultures developed in the presence of glial cells (GM, grey,  $n = 9$ ). Right, facilitation recovered exponentially, illustrated as paired pulse ratio plotted against time. SCM and GM showed time constants of  $41 \text{ ms}$  and  $28 \text{ ms}$ , respectively. *B*, left, the degree of PPF was increased both in SCM ( $n = 8$ ) and GM ( $n = 6$ ) by lowering  $[\text{Ca}^{2+}]_o$  to  $0.5 \text{ mM}$ . In this condition, PPF recovered more slowly, showing time constants of  $0.6 \text{ s}$  and  $0.72 \text{ s}$  in SCM and GM, respectively. Error bars indicate s.e.m. Each point shows the average of values obtained in  $\geq 5$  different cells.

Regehr, 2002). The time required to refill the RRP after depression depends on vesicle supply from cytoplasmic pools and the speed of endocytosis (Rizzoli & Betz, 2005). The time course of depression assayed by a paired pulse protocol changed from a fast mono-exponential process in single cell microcultures to a longer lasting bi-exponential time course in glial microcultures. A plausible explanation for this change in behaviour was the enhanced frequency of mEPSCs observed in glial microcultures. If mEPSCs originated from vesicles of the RRP (Rosenmund & Stevens, 1996), the enhanced spontaneous synaptic activity of glial microcultures (almost an order of magnitude larger than single cell microcultures) would antagonize the refilling process, and thus cause a longer lasting depression. Why was depression but not facilitation modified in glial microcultures? Despite the molecular mechanisms involved in facilitation and depression seeming to be different (Zucker & Regehr, 2002), facilitation can only be supported if the RRP comprises enough vesicles. Facilitation was observed at low release probabilities, when a small fraction of the RRP was mobilized. In addition, facilitation and depression shared a common feature: they were inversely related to the number of vesicles released from the RRP by a single action potential (Fig. 7B). Following the assumption that mEPSCs originated from RRP vesicles, the present data suggest that their spontaneous secretion did not compromise the capacity of available quanta for release in low probability conditions, and therefore did not modify the time course of facilitation. Previous studies already showed that glial cells enhance the frequency of spontaneous neurotransmission in synapses formed by retinal ganglion cells (Pfrieger & Barres, 1997) or spinal motor neurons (Ullian *et al.* 2004). The similar observations presented suggest that this might be a common property of glial cells, and particularly Schwann cells.

In sympathetic ganglia thin lamellae of Schwann cell processes cover many nicotinic synapses, preganglionic endings, and somatic and dendritic surfaces (Gibbins & Morris, 2006). So far the reason for such arrangements among Schwann cells, preganglionic boutons and target neurons is still unknown. Present data indicate that the particular morphology and distribution of glia is key to their ability to modify short-term plasticity. Other types of glial cells, such as Schwann cells in motor axons, Bergmann glia in the cerebellum, or astrocytes, cover synapses, and sense and modulate synaptic activity (Bergles *et al.* 1997; Araque *et al.* 1998; Robitaille, 1998). It is likely that a restricted morphological arrangement is required for the observed effect of Schwann cells on synaptic plasticity. In such a narrow environment, diffusible molecules could mediate a crosstalk, similarly to the action of NO or glutamate at the neuromuscular junction (Thomas & Robitaille, 2001; Pinard *et al.* 2003). Future experiments

are required to establish the identity of the molecular mechanism mediating the increase in the frequency of mEPSCs evoked by Schwann cells.

Nicotinic synapses in ganglia show variable strengths *in vivo*, producing postsynaptic responses that can be supra-threshold or strong and subthreshold or weak. Previous studies have considered convergence of preganglionic fibres to be a key factor determining such responses and therefore controlling the firing of postganglionic sympathetic neurons (McLachlan *et al.* 1997). Plasticity of individual synapses, however, should be taken into account. Changes in synaptic strength in sympathetic ganglia occur during long-term potentiation, whose primary physiological implication is an enhancement of tonic efferent impulses to neuroeffector organs (Alkadhi *et al.* 2005). The observed short-term depression indicates the ability of preganglionic synapses to act as low pass filters. The present data show that Schwann cells play a modulator role in this process: by enhancing the frequency of mEPSCs they decrease the band-pass of the filter. Glial cells would therefore exert a maturation effect on synapses, conferring exclusive properties on neurons, at least in *in vitro* conditions. Such an action would provide a fine tuning of those functions controlled by the superior cervical ganglion, as for example blood vessel tone (Gerges *et al.* 2002). Altogether, the present work evidences that the cellular environment plays a key role in determining synaptic strength of ganglionic neurotransmission, but more experiments are required to establish the mechanisms governing synaptic strength of ganglionic nicotinic synapses.

## References

- Alkadhi KA, Alzoubi KH & Aleisa AM (2005). Plasticity of synaptic transmission in autonomic ganglia. *Prog Neurobiol* **75**, 83–108.
- Araque A, Parpura V, Sanzgiri RP & Haydon PG (1998). Glutamate-dependent astrocyte modulation of synaptic transmission between cultured hippocampal neurons. *Eur J Neurosci* **10**, 2129–2142.
- Assouline JG, Bosch P, Lim R, Kim IS, Jensen R & Pantazis NJ (1987). Rat astrocytes and Schwann cells in culture synthesize nerve growth factor-like neurite-promoting factors. *Brain Res* **428**, 103–118.
- Baluk P (1995). Structure of autonomic ganglia. In *Autonomic Ganglia*, ed. McLachlan EM, pp. 13–72. Informa Health Care.
- Bampton ET & Taylor JS (2005). Effects of Schwann cell secreted factors on PC12 cell neuritogenesis and survival. *J Neurobiol* **63**, 29–48.
- Bekkers JM & Stevens CF (1991). Excitatory and inhibitory autaptic currents in isolated hippocampal neurons maintained in cell culture. *Proc Natl Acad Sci U S A* **88**, 7834–7838.
- Bekkers JM & Stevens CF (1996). Cable properties of cultured hippocampal neurons determined from sucrose-evoked miniature EPSCs. *J Neurophysiol* **75**, 1250–1255.

- Bergles DE, Dzuby JA & Jahr CE (1997). Glutamate transporter currents in bergmann glial cells follow the time course of extrasynaptic glutamate. *Proc Natl Acad Sci U S A* **94**, 14821–14825.
- Birks RI & Isacoff EY (1988). Burst-patterned stimulation promotes nicotinic transmission in isolated perfused rat sympathetic ganglia. *J Physiol* **402**, 515–532.
- Christopherson KS, Ullian EM, Stokes CC, Mallowney CE, Hell JW, Agah A, Lawler J, Moshier DF, Bornstein P & Barres BA (2005). Thrombospondins are astrocyte-secreted proteins that promote CNS synaptogenesis. *Cell* **120**, 421–433.
- Chun LL & Patterson PH (1977). Role of nerve growth factor in the development of rat sympathetic neurons in vitro. I. Survival, growth, and differentiation of catecholamine production. *J Cell Biol* **75**, 694–704.
- Cocchia D & Michetti F (1981). S-100B antigen in satellite cells of the adrenal medulla and the superior cervical ganglion of the rat. An immunochemical and immunocytochemical study. *Cell Tissue Res* **215**, 103–112.
- Crowley C, Spencer SD, Nishimura MC, Chen KS, Pitts-Meek S, Armanini MP, Ling LH, McMahon SB, Shelton DL, Levinson AD *et al.* (1994). Mice lacking nerve growth factor display perinatal loss of sensory and sympathetic neurons yet develop basal forebrain cholinergic neurons. *Cell* **76**, 1001–1011.
- Deitmer JW & Rose CR (1996). pH regulation and proton signalling by glial cells. *Prog Neurobiol* **48**, 73–103.
- Dittman JS & Regehr WG (1998). Calcium dependence and recovery kinetics of presynaptic depression at the climbing fiber to Purkinje cell synapse. *J Neurosci* **18**, 6147–6162.
- Dodge FA Jr & Rahamimoff R (1967). Co-operative action of calcium ions in transmitter release at the neuromuscular junction. *J Physiol* **193**, 419–432.
- Forehand CJ (1985). Density of somatic innervation on mammalian autonomic ganglion cells is inversely related to dendritic complexity and preganglionic convergence. *J Neurosci* **5**, 3403–3408.
- Freschi JE (1982). Effect of serum-free medium on growth and differentiation of sympathetic neurons in culture. *Brain Res* **256**, 455–464.
- Furshpan EJ, Landis SC, Matsumoto SG & Potter DD (1986b). Synaptic functions in rat sympathetic neurons in microcultures. I. Secretion of norepinephrine and acetylcholine. *J Neurosci* **6**, 1061–1079.
- Furshpan EJ, Potter DD & Matsumoto SG (1986a). Synaptic functions in rat sympathetic neurons in microcultures. III. A Purinergic effect on cardiac myocytes. *J Neurosci* **6**, 1099–1107.
- Gerges NZ, Aleisa AM, Alhaider AA & Alkadhi KA (2002). Reduction of elevated arterial blood pressure in obese Zucker rats by inhibition of ganglionic long-term potentiation. *Neuropharmacology* **43**, 1070–1076.
- Gibbins IL & Morris JL (2006). Structure of peripheral synapses: autonomic ganglia. *Cell Tissue Res* **326**, 205–220.
- Goda Y & Stevens CF (1998). Readily releasable pool size changes associated with long term depression. *Proc Natl Acad Sci U S A* **95**, 1283–1288.
- Huang WX, Yu Q & Cohen MI (2000). Fast (3 Hz and 10 Hz) and slow (respiratory) rhythms in cervical sympathetic nerve and unit discharges of the cat. *J Physiol* **523**, 459–477.
- Johnson MI, Ross CD, Meyers M, Spitznagel EL & Bunge RP (1980). Morphological and biochemical studies on the development of cholinergic properties in cultured sympathetic neurons. I. Correlative changes in choline acetyltransferase and synaptic vesicle cytochemistry. *J Cell Biol* **84**, 680–691.
- Kofuji P & Newman EA (2004). Potassium buffering in the central nervous system. *Neuroscience* **129**, 1045–1056.
- Mains RE & Patterson PH (1973). Primary cultures of dissociated sympathetic neurons. I. Establishment of long-term growth in culture and studies of differentiated properties. *J Cell Biol* **59**, 329–345.
- Mathey E & Armati PJ (2007). Introduction to the Schwann cell. In *The Biology of Schwann Cells: Development, Differentiation and Immunomodulation*, ed. Armati PJ, pp. 1–12. Cambridge University Press, Cambridge.
- McCann CM & Lichtman JW (2008). In vivo imaging of presynaptic terminals and postsynaptic sites in the mouse submandibular ganglion. *Dev Neurobiol* **68**, 760–770.
- McLachlan EM, Davies PJ, Habler HJ & Jamieson J (1997). On-going and reflex synaptic events in rat superior cervical ganglion cells. *J Physiol* **501**, 165–181.
- Mennerick S & Zorumski CF (1994). Glial contributions to excitatory neurotransmission in cultured hippocampal cells. *Nature* **368**, 59–62.
- Millar AG, Bradacs H, Charlton MP & Atwood HL (2002). Inverse relationship between release probability and readily releasable vesicles in depressing and facilitating synapses. *J Neurosci* **22**, 9661–9667.
- Mochida S, Nonomura Y & Kobayashi H (1994). Analysis of the mechanism for acetylcholine release at the synapse formed between rat sympathetic neurons in culture. *Microsc Res Tech* **29**, 94–102.
- Moulder KL & Mennerick S (2005). Reluctant vesicles contribute to the total readily releasable pool in glutamatergic hippocampal neurons. *J Neurosci* **25**, 3842–3850.
- Murthy VN, Sejnowski TJ & Stevens CF (1997). Heterogeneous release properties of visualized individual hippocampal synapses. *Neuron* **18**, 599–612.
- Nagler K, Mauch DH & Pfrieger FW (2001). Glia-derived signals induce synapse formation in neurones of the rat central nervous system. *J Physiol* **533**, 665–679.
- Oger J, Arnason BG, Pantazis N, Lehrich J & Young M (1974). Synthesis of nerve growth factor by L and 3T3 cells in culture. *Proc Natl Acad Sci U S A* **71**, 1554–1558.
- Otsu Y, Shahrezaei V, Li B, Raymond LA, Delaney KR & Murphy TH (2004). Competition between phasic and asynchronous release for recovered synaptic vesicles at developing hippocampal autaptic synapses. *J Neurosci* **24**, 420–433.
- Pfrieger FW & Barres BA (1997). Synaptic efficacy enhanced by glial cells in vitro. *Science* **277**, 1684–1687.
- Pinard A, Levesque S, Vallee J & Robitaille R (2003). Glutamatergic modulation of synaptic plasticity at a PNS vertebrate cholinergic synapse. *Eur J Neurosci* **18**, 3241–3250.
- Rizzoli SO & Betz WJ (2005). Synaptic vesicle pools. *Nat Rev Neurosci* **6**, 57–69.

- Robitaille R (1998). Modulation of synaptic efficacy and synaptic depression by glial cells at the frog neuromuscular junction. *Neuron* **21**, 847–855.
- Rohrer H & Sommer I (1983). Simultaneous expression of neuronal and glial properties by chick ciliary ganglion cells during development. *J Neurosci* **3**, 1683–1693.
- Rosenmund C & Stevens CF (1996). Definition of the readily releasable pool of vesicles at hippocampal synapses. *Neuron* **16**, 1197–1207.
- Saadat S, Sendtner M & Rohrer H (1989). Ciliary neurotrophic factor induces cholinergic differentiation of rat sympathetic neurons in culture. *J Cell Biol* **108**, 1807–1816.
- Schluter OM, Basu J, Sudhof TC & Rosenmund C (2006). Rab3 superprimes synaptic vesicles for release: implications for short-term synaptic plasticity. *J Neurosci* **26**, 1239–1246.
- Schneggenburger R, Meyer AC & Neher E (1999). Released fraction and total size of a pool of immediately available transmitter quanta at a calyx synapse. *Neuron* **23**, 399–409.
- Stevens CF & Williams JH (2007). Discharge of the readily releasable pool with action potentials at hippocampal synapses. *J Neurophysiol* **98**, 3221–3229.
- Thomas S & Robitaille R (2001). Differential frequency-dependent regulation of transmitter release by endogenous nitric oxide at the amphibian neuromuscular synapse. *J Neurosci* **21**, 1087–1095.
- Trouslard J, Marsh SJ & Brown DA (1993). Calcium entry through nicotinic receptor channels and calcium channels in cultured rat superior cervical ganglion cells. *J Physiol* **468**, 53–71.
- Ullian EM, Harris BT, Wu A, Chan JR & Barres BA (2004). Schwann cells and astrocytes induce synapse formation by spinal motor neurons in culture. *Mol Cell Neurosci* **25**, 241–251.
- Zhang JM, Wang HK, Ye CQ, Ge W, Chen Y, Jiang ZL, Wu CP, Poo MM & Duan S (2003). ATP released by astrocytes mediates glutamatergic activity-dependent heterosynaptic suppression. *Neuron* **40**, 971–982.
- Zucker RS & Regehr WG (2002). Short-term synaptic plasticity. *Annu Rev Physiol* **64**, 355–405.

### Acknowledgements

A.L. is a Miguel Servet Researcher from the Servicio Nacional de Salud (Spain). This work was supported by grants PI-05-1050 and FIS-04-173 from Instituto de Salud Carlos III.

### Supplemental material

Online supplemental material for this paper can be accessed at: <http://jp.physoc.org/cgi/content/full/jphysiol.2008.160044/DC1>